

# Atmospheric plasma jets for generation of nanostructured materials or nanoparticles

Jan Benedikt<sup>1</sup>, Ove Hansen<sup>1</sup>, Oleksandr Polonskyi<sup>2</sup>, Sadegh Askari<sup>1</sup>, Judith Golda<sup>1</sup>

<sup>1</sup> Institute of Experimental and Applied Physics, Kiel University, Germany

<sup>2</sup> Institute for Material Science, Kiel University, Germany

**Abstract:** Cold atmospheric plasmas are source of high reactivity. They can be effectively uses for dissociation of precursor gases, where the reactive species can be applied in surface treatment or in generation of nanoparticles and nanostructured thin films. In this contribution we report on the rf-driven atmospheric plasma jet with dielectric on the electrodes, which can be operated at large applied powers and elevated gas temperature. The controlled formation of ultra-small (< 4 nm) silicon nanoparticles and oxidation of metal films with formation of nanostructures will be presented and discussed.

**Keywords:** Cold atmospheric plasmas, nanoparticles, nanomaterials.

## 1. Introduction

Atmospheric non-equilibrium plasmas can generate high densities of reactive species or dissociate effectively precursor gases. Contrary to low-pressure plasmas, the collisions prevent ion bombardment and the diffusion is slow as transport mechanism. On the other hand, energy can be effectively stored in form of excitation energy (metastable atoms, excimers, metastable molecules such as  $N_2(A)$ ) and a convection can be used as an effective transport of reactive species in atmospheric plasma jets. However, the main application of atmospheric plasmas is mainly in surface treatment applications, they are not widely used in applications for thin film generation or etching due to the limited quality of the deposited material, missing ion bombardment and only localized treatment. Their potentials in material synthesis are mainly demonstrated in proof of principle experiments [1], where the formation of nanostructured materials [2,3] or nanoparticles [4] is especially interesting.

## 2. Experimental Setup

The experiments are performed with atmospheric plasma sources based in design on a so-called COST reference jet [5] with two metal electrode at the distance of 1 mm and with capacitive coupling of the rf-power, which generates cold plasma in He with small admixture of reactive gas. As a new element, we use a glass capillary with round, square, or rectangular cross section in between the electrodes (with variable distance down to 0.2 mm) to guide the gas flow (see Fig. 1).

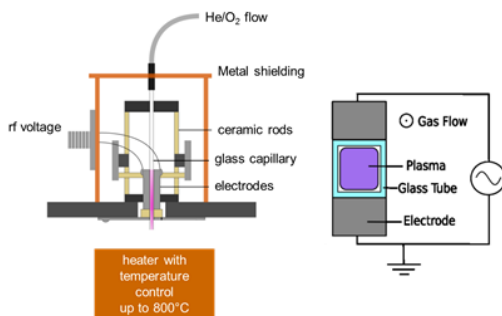


Fig. 1. Scheme of the experimental setup. The inner cross-section of the glass capillary is  $1 \times 1 \text{ mm}^2$ .

The capillary as dielectrics allows much larger power being applied to the plasma without development of electric arc and resulting electrode damage as otherwise observed with the COST reference jet. Still, high-applied power leads to a formation of a contracted  $\gamma$ -like mode, where the main ionisation and excitation region is located at the dielectric in front of the electrodes. The absorbed power in the plasma as obtained from the measurements of calibrated volt and current probes is shown in Fig. 2 and clearly demonstrate the transition from the volumetric ( $\alpha$ -mode) discharge to contracted discharge at transition root-mean-square voltage around 450 V.

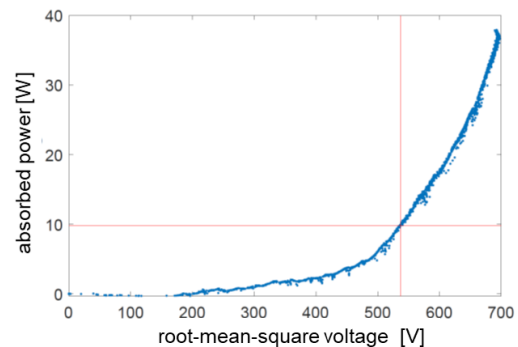


Fig. 2. Measured absorbed power as a function of applied root-mean-square voltage.

The contracted mode can be operated for long time (no damage or change observed after weeks of operation). The gas temperature, which is around  $40 \text{ }^\circ\text{C}$  in the  $\alpha$ -mode, rises to  $400 \text{ }^\circ\text{C}$  in the contracted mode as measured with a thermocouple at the capillary exit. The  $O_2$  dissociation degree is around 10% in the  $\alpha$ -mode and it is expected that this value will be closed to 100% in the contracted mode due to higher plasma density, promoting electron impact dissociation, and higher gas temperature, which slows down or even prevents recombination reactions. Mass spectrometry measurements are being prepared to measure the  $O_2$  dissociation degree and O atom density. Additionally, the higher gas temperature supports formation of crystalline semiconductor nanoparticles (e.g.

from SiH<sub>4</sub> precursor). The plasma is analysed by means of molecular beam mass spectrometry (MBMS) and optical emission spectroscopy (OES) and the generated material is characterised by Fourier transform infrared spectroscopy (FTIR), scanning electron microscopy (SEM), X-ray photoelectron spectroscopy (XPS), and transmission electron microscopy (TEM). Additionally, the size of the generated NPs is determined by 1 nm scanning mobility particle sizer (1 nm SMPS).

### 3. Results and Discussion

#### Generation of silicon nanoparticles

Silicon nanoparticles (Si-NPs) has been generated with the excellent size selectivity from He/Ar/SiH<sub>4</sub> gas mixture as demonstrated in Fig. 3.

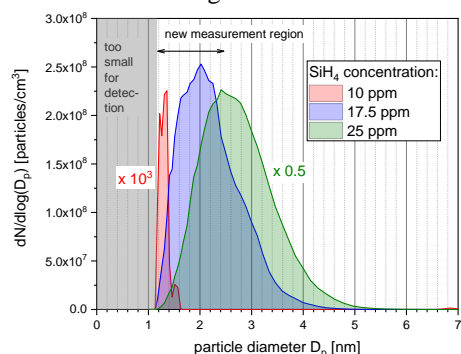


Fig. 3. Analysis of the SiH<sub>4</sub>-concentration effects on negatively charged particle size distribution functions as generated in He/Ar/SiH<sub>4</sub> plasma. Experimental conditions: He flow 500 sccm, Ar/0.01%SiH<sub>4</sub> flow varied, voltage frequency 13.56 MHz, capillary inner diameter 0.7 mm, electrode length 40 mm.

The flexibility of the atmospheric plasmas and the ability to measure particle size distributions down to 1.2 nm allows the generation of nanoparticles or nanocrystals with tuned size, composition and surface passivation.

#### Treatment of metal surfaces

The oxidation of the metallic surface is utilised in the treatment of thin copper foils by contracted discharge in He/O<sub>2</sub> gas mixture at variety of substrate temperatures (100°C – 800°C). The morphology of treated copper film has been analysed with scanning electron microscopy (SEM) as function of surface temperature, time, and O<sub>2</sub> concentration. Fig. 4 shows an example of the surface morphology under the running jet with O atoms being involved in the treatment and at the region far away from the jet axis, where the thermal oxidation at the same temperature took place. It is clearly visible that the treatment with O atoms leads to formation of vertical nano walls, which are not observed in the thermal treatment. The non-equilibrium conditions resulting from the enhanced O<sub>2</sub> dissociation and presence of O atoms result very probably in enhanced mobility of oxygen along the surface providing conditions for formation of unique nanostructures. It should be noted that similar structures

are observed at 100°C (no oxidation) and at 800°C (the similar structure of large oxide grains). The XPS measurement revealed in both cases the presence of more stable cupric oxide CuO. Similar observations have been obtained previously by Altaweel et al. [2] under microwave atmospheric plasma jet without the control of the surface temperature.

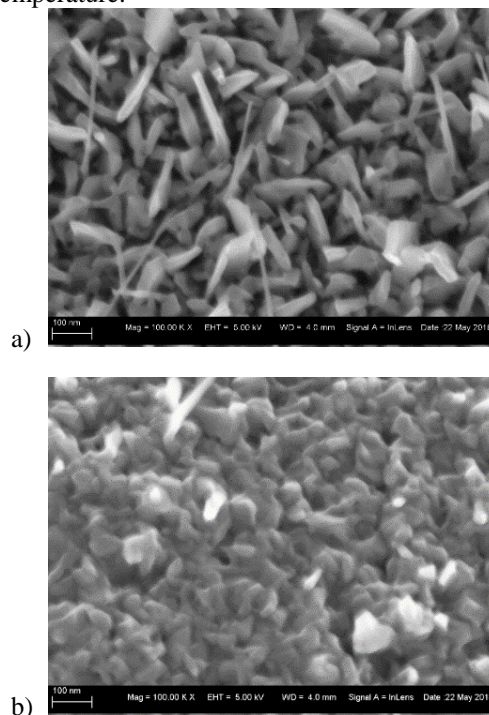


Fig. 4. SEM image of the surface of copper oxide after 60 minutes of treatment with a) plasma afterglow with O atoms and b) with He/O<sub>2</sub> gas. Conditions: He flow 1 slm, O<sub>2</sub> flow 5 sccm, applied rf-power 50 W, absorbed plasma power 10 W.

### 4. Conclusions

The rf-driven atmospheric plasma jet can be continuously operated in contracted mode and used for generation of ultra-small nanoparticles or generation of nanostructured oxide films. The surface treatment of metallic layers leads to nanostructured oxidation with different morphology compared to thermal oxidation. The aim of this and following study is to provide fundamental understanding of nanoparticle formation and surface reactions involved in the oxidation process.

### 5. References

- [1] D. Mariotti, T. Belmonte, J. Benedikt, T. Velusamy, G. Jain, V. Svrcek, *Plasma Process Polym* **13**, 70–90 (2016).
- [2] A. Altaweel, G. Filipič, T. Gries, T. Belmonte, *J. Cryst. Growth* **407**, 17 (2014).
- [3] D. Mariotti, K. Ostrikov K, *J. Phys. D: Appl. Phys.* **42**, 092002 (2009).
- [4] S. Askari, V. Svrcek, P. Maguire, D. Mariotti, *Adv. Mater.* **27** 8011 (2015).
- [5] J. Golda et al., *J. Phys. D: Appl. Phys.* **49**, 084003 (2016).